

Theory of Photothermal Displacement Method for Determining Physical Properties of Multilayered Coatings

T. Elperin · G. Rudin

Received: 25 February 2009 / Accepted: 17 August 2009 / Published online: 29 August 2009
© Springer Science+Business Media, LLC 2009

Abstract In this study theoretical principles underlying the photothermal method for determining thermal properties of opaque multilayered and functionally graded coatings are analyzed. The method is based on irradiation of the assembly by the repetitive pulse of focused laser radiation that is absorbed in the subsurface region and causes non-uniform heating and buckling of a coating. The irradiated surface of a coating is monitored by a low power beam of a second laser that is reflected from the specimen. The deflection angle of the monitoring beam, as a function of time, contains the relaxation and the “wave” components. It is shown that the phase of the “wave” component depends on the thermophysical properties (e.g., thermal diffusivity or thermal conductivity) of a coating. These properties can be determined by comparing experimentally measured values of the phase shift of the “wave” component with the theoretical values obtained from the analytical solution of the two-dimensional thermal elasticity problem for a multilayered coating–substrate assembly.

Keywords Laser heating · Multilayer coating · Phase shift

Nomenclature

- a Thermal diffusivity
- c Specific heat
- G Shear modulus

T. Elperin (✉) · G. Rudin
Department of Mechanical Engineering, Pearlstone Center for Aeronautical Engineering Studies,
Ben-Gurion University of the Negev, P.O. Box 653, Beer Sheva 84105, Israel
e-mail: elperin@bgu.ac.il

G. Rudin
e-mail: rudin@bgu.ac.il

I_0	Laser beam power absorbed by a coating
$I(t)$	Laser beam power
$J_i(x)$	i th order Bessel function of the first kind
r	Radial coordinate
r_0	Radius of a laser beam
s, p	Parameters of Laplace–Hankel transforms with respect to t and r , respectively
t	Time
T	Temperature
$\bar{T}(s, p, z)$	Laplace–Hankel transform of temperature
w	Axial components of displacement
z	Axial coordinate
α	Coefficient of linear thermal expansion
Δ	Coating thickness
ε	Monitoring beam deflection angle
λ	Thermal conductivity
ν	Poisson's ratio
σ_0	Optical absorption coefficient
τ_0	Duration of a single laser pulse
ω	Modulation cyclic frequency of a power laser beam
$\Delta\Phi$	Phase shift

Subscripts

0	Substrate
g	Air
$k = 1, \dots, n$	Number of a layer in a coating
m	Number of harmonics

1 Introduction

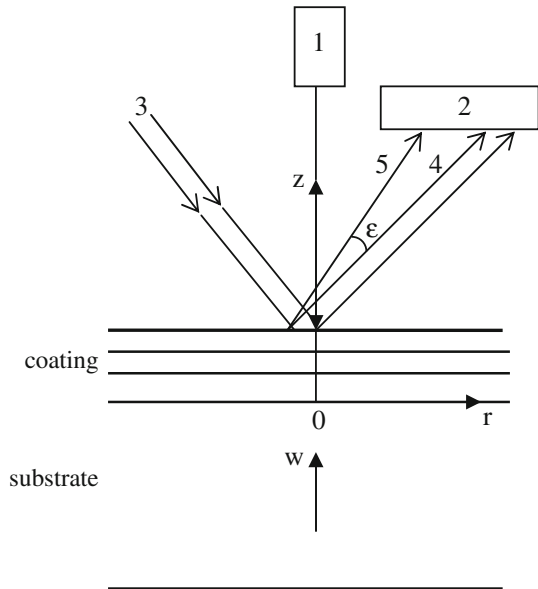
The determination of physical properties of thin coatings, interlayers, and interfaces is required in many fields of technology, e.g., electronics, design of advanced functionally graded materials, optics, etc. The photothermal method is used for measuring physical characteristics and has a number of advantageous properties over the traditional methods, e.g., absence of mechanical contact with the investigated sample, ability to distinguish surface and bulk characteristics, and high accuracy of measurements of the optical and thermal properties of solids. This method is based on local heating of the investigated sample by modulated radiation of a power laser. The absorbed electromagnetic radiation is converted into heat and causes a local increase of temperature and generation of thermal waves in an illuminated specimen. The amplitude and the phase of these thermal waves depend on the thermophysical properties of a specimen, properties of surfaces and interfaces, and the presence of subsurface defects and cracks. There are a number of photothermal techniques for measuring physical properties of materials (for an overview of the photothermal techniques, see [1]), e.g.,

photothermal displacement spectroscopy [2–5], photoacoustic spectroscopy [6–8], photothermal radiometry [9, 10], and the “mirage effect” associated with deflection of the monitoring beam caused by a gradient of the refractive index of air in the vicinity of the heated surface [11, 12]. A limitation of the latter method is that the optical characteristics, e.g., absorption coefficient of the heated surface and physical properties of the surrounding air influence the measured parameters of the monitoring beam. In contrast to this, the photothermal displacement method is not sensitive to the optical characteristics of the heated surface. The incident angle of the monitoring beam can be chosen sufficiently small so that the effect of the gradient of the refractive index of air on the deflected beam can be neglected.

In this study we explore theoretically the feasibility of using the photothermal displacement method for determining thermal characteristics of a thin coating deposited on a substrate (no experimental results are reported). This method has some advantageous properties in comparison with the above described photothermal methods [2], especially high sensitivity to the variations of the physical characteristics of the thin coatings. The physical basis for this method is local heating of a coating by a repetitive pulse of a power laser that causes non-uniform deformation (buckling) of a coating and a substrate. The heated region of a coating is monitored by a narrow low power beam (monitoring beam) of a second laser that is reflected from a coating and does not heat a specimen. Because of a non-stationary buckling of a surface, the reflected monitoring beam alternates between paths 4 and 5 (see Fig. 1), and the system operates as a convex “thermal mirror” [13] with a time-dependent focal distance, i.e., as a quasi-optical system that is formed by local heating of a coating. We suggest using two parallel monitoring beams in order to minimize the influence of the heated air in the vicinity of the heated coating on the beam deflection angle (“mirage effect”). The distance between two parallel beams is chosen in the range $(1-2)r_0$ in order to obtain the maximum values of the deflection angle ε . In this case the temperature difference between the locations where two beams are reflected from the sample is small, and the changes of the deflection angles of two beams induced by heated air are nearly the same. Consequently, the contribution of the “mirage effect” to the measured difference $|\varepsilon_1 - \varepsilon_2|$ can be considerably reduced.

In the previous study [13] we proposed an algorithm of the “thermal mirror” method for determining physical properties of multilayered coatings. The method is based on irradiation of a coating by a short *single* pulse of a power laser and measurement of the temporal relaxation of the monitoring beam deflection angle ε . In the present study we suggest using the *repetitive* pulses (with a frequency ω) of a power laser for heating the investigated assembly. In this case the deflection angle ε that is registered in the experiment, contains the relaxation ε_{rel} (the principal measured parameter in [13]) and the “wave” ε_w components. The component ε_{rel} is caused by the transient diffusion of thermal energy from the coating into the substrate and the component ε_w (the principal measured parameter in the present study) arises due to the modulated heating of the coating. The obtained signal can be expanded in a Fourier series which comprise harmonics with the frequencies $\omega, 2\omega, 3\omega, \dots$. In this manner using the repetitive pulses we obtain the response of the quasi-optical system in a wide range of frequencies. Comparing experimentally measured phase data of the “wave” component

Fig. 1 Schematics of the photothermal displacement method. 1—heating laser beam; 2—position sensor; 3—splitted monitoring laser beam; 4, 5—reflected monitoring beam before and after heating by a power laser beam



with the theoretically predicted values obtained from solution of the non-stationary two-dimensional thermal elasticity problem allows determination of the thermal characteristics of a thin coating. The sensitivity of the phase data of the component ϵ_w to variations of thermophysical characteristics of a coating is significantly higher than the sensitivity of the amplitude data, i.e., the phase of ϵ_w is more important, in comparison with the amplitude, for experimental determination of thermal properties.

The photothermal method can be used also in the case of a coating manufactured from a functionally graded material (FGM). The FGM coatings are prepared by the “layer by layer” method whereby the volumetric content of the ceramics (e.g., WC, ZrO₂) changes from layer to layer in order to produce the desired gradient of physical properties in a normal direction. The photothermal method can be used for determining thermophysical properties after deposition of each individual layer (i.e., layer by layer), until completion of the formation of a coating.

2 Solution of Equations of Thermal Elasticity

Consider an opaque coating–substrate assembly heated by repetitive pulses of a power laser beam propagating in a direction normal to the coating. The temperature distribution $T_k(r, z, t)$ in a multilayer coating–substrate assembly is governed by a non-stationary two-dimensional heat conduction equation:

$$c_k \frac{\partial T_k}{\partial t} = \lambda_k \left[\frac{1}{r} \frac{\partial}{\partial r} \left(r \frac{\partial T_k}{\partial r} \right) + \frac{\partial^2 T_k}{\partial z^2} \right]. \tag{1}$$

The initial and “far-field” boundary conditions to Eq. 1 read

$$T_k|_{t=0} = \frac{\partial T_k}{\partial r} \Big|_{r \rightarrow \infty} = \frac{\partial T_k}{\partial z} \Big|_{z \rightarrow \pm \infty} = 0, \quad (k = 0, 1, \dots, n). \quad (2)$$

The “external” boundary condition at the irradiated surface ($k = n$) that is exposed to the air is as follows:

$$T_n = T_g, \quad \lambda_n \frac{\partial T_n}{\partial z} - \lambda_g \frac{\partial T_g}{\partial z} = I_0 \sigma_0 \exp\left(-\frac{r^2}{r_0^2}\right) f(t). \quad (3)$$

These initial and boundary conditions must be supplemented by temperature and heat flux continuity conditions at the interface $z = \Delta_k$ ($k = 0$ for a substrate):

$$T_k = T_{k+1}, \quad \lambda_k \frac{\partial T_k}{\partial z} = \lambda_{k+1} \frac{\partial T_{k+1}}{\partial z}, \quad (4)$$

where

$$f(t) = \begin{cases} 1, & 0 < t < \tau_0, \\ 0, & \tau_0 < t < \tau_0 + \tau, \end{cases} \quad f(t) = f[t + i(\tau_0 + \tau)], \quad i = 1, 2, \dots \quad (5)$$

is a periodic function with a period $(\tau + \tau_0)$, and σ_0 is a surface absorption coefficient of the coating. It is assumed that the coating is optically thick ($\sigma_0 \Delta_n \gg 1$) since the absorption length is small in comparison with its thickness. In a previous study [13], we obtained the solution of the thermal conductivity problem for an opaque coating–substrate assembly heated by a short *single* pulse of a power laser beam in the case of a small Fourier number, $Fo = a_n t / \Delta^2 \ll 1$. In the present study an investigated assembly is heated by *repetitive* pulses of a power laser beam and solution of the heat conduction problem is obtained without any limitation on the Fourier number.

Applying the Laplace–Hankel transform to Eqs. 1–5, we obtain the following equations:

$$\frac{d^2 \bar{T}_k}{dz^2} = \left(\frac{s}{a_k} + p^2\right) \bar{T}_k, \quad (6)$$

$$\bar{T}_k|_{t=0} = \frac{\partial \bar{T}_k}{\partial r} \Big|_{r \rightarrow \infty} = \frac{\partial \bar{T}_0}{\partial z} \Big|_{z = -\infty} = 0, \quad (7)$$

$$\lambda_n \frac{\partial \bar{T}_n}{\partial z} - \lambda_g \frac{\partial \bar{T}_g}{\partial z} = \frac{I_0 \sigma_0 r_0^2}{2} \times \exp\left(-p^2 r_0^2 / 4\right) \bar{f}(s)$$

at the surface of a coating ($z = \Delta_n$),

$$\bar{T}_0 = \bar{T}_1, \quad \lambda_1 \frac{\partial \bar{T}_1}{\partial z} = \lambda_0 \frac{\partial \bar{T}_0}{\partial z} \quad (8)$$

at $z = 0$,

$$\bar{T}_k = \bar{T}_{k+1}, \quad \lambda_k \frac{\partial \bar{T}_k}{\partial z} = \lambda_{k+1} \frac{\partial \bar{T}_{k+1}}{\partial z}, \tag{9}$$

and

$$\bar{f}(s) = \frac{1 - \exp(s\tau_0)}{s} \sum_{n=0}^{\infty} \exp[-ns(\tau_0 + \tau)] = \frac{1 - \exp(-s\tau_0)}{s \{1 - \exp[-s(\tau_0 + \tau)]\}}, \tag{10}$$

where

$$\begin{aligned} \bar{T}_i(s, p, z) &= \int_0^{\infty} \int_0^{\infty} T_i(t, r, z) \exp(-st) r J_0(pr) dt dr, \\ \bar{f}(s) &= \int_0^{\infty} f(t) \exp(-st) dt. \end{aligned} \tag{11}$$

The general solution of Eq. 6 reads

$$\bar{T}_{n+1} = M_{n+1} \exp(-\gamma_{n+1}z) \tag{12}$$

in the air above a coating,

$$\bar{T}_k = M_k \exp(-\gamma_k z_k) + N_k \exp(\gamma_k z_k) \tag{13}$$

in the multilayered coating, $0 < z_k < \Delta_k, \quad k = 1, 2, 3, \dots, n$;

$$\bar{T}_0 = N_0 \exp(\gamma_0 z) \tag{14}$$

in the substrate. Here $\gamma_k = \sqrt{\frac{s}{a_k} + p^2}$, N_0, M_k, N_k , and M_{n+1} are integration constants.

We use the recursion procedure for determining these integration constants. To this end, let us represent the integration constants in the following form:

$$M_k = A_k N_0 \bar{f}(s), \quad N_k = B_k N_0 \bar{f}(s). \tag{15}$$

Using the continuity conditions of Eq. 9 for temperature and heat flux, we obtain the expressions for the coefficients A_1, B_1 in the layer of a coating adjacent to a substrate ($k = 1$):

$$A_1 = \frac{1}{2} \left(1 - \frac{\lambda_0 \gamma_0}{\lambda_1 \gamma_1} \right), \quad B_1 = \frac{1}{2} \left(1 + \frac{\lambda_0 \gamma_0}{\lambda_1 \gamma_1} \right). \quad (16)$$

Substituting Eq. 15 into the continuity conditions of Eq. 9 for $k > 1$ yields the following recursive relations:

$$A_k = \lambda_{k-1}^+ \exp(-\mu_{k-1}) A_{k-1} + \lambda_{k-1}^- \exp(\mu_{k-1}) B_{k-1}, \quad (17)$$

$$B_k = \lambda_{k-1}^- \exp(-\mu_{k-1}) A_{k-1} + \lambda_{k-1}^+ \exp(\mu_{k-1}) B_{k-1}, \quad (18)$$

$$\mu_k(s) = \gamma_k \Delta_k, \quad \lambda_{k-1}^\pm = \frac{1}{2} \left(1 \pm \frac{\lambda_{k-1} \gamma_{k-1}}{\lambda_k \gamma_k} \right). \quad (19)$$

The boundary condition at the surface of a coating after substitution of Eqs. 17–19 yields

$$N_0(p, s) = \frac{I_0 \sigma_0 r_0^2 \Delta_n \exp(-p^2 r_0^2 / 4)}{2 \lambda_n \mu_n [-A_n \lambda_g^- \exp(-\mu_n) + B_n \lambda_g^+ \exp(\mu_n)]}, \quad (20)$$

where $\lambda_g^\pm = \frac{1}{2} \left(1 \pm \frac{\lambda_g \gamma_g}{\lambda_n \gamma_n} \right)$.

Substituting Eqs. 15–20 into Eqs. 12–14 allows determination of the Laplace–Hankel transform of the temperature distribution in the assembly that is used further for solution of the two-dimensional equations of thermal elasticity.

Expression for the monitoring beam deflection angle is based on the solution of the equations of thermal elasticity which have been obtained in our previous study (for details, see [13]):

$$\begin{aligned} \bar{\varepsilon}(r, s) = 2 \left. \frac{\partial \bar{w}}{\partial r} \right|_{z=\Delta_n} = 4\alpha_0 (1 + \nu) \int_0^\infty \left\{ \bar{\theta}_0(p) + \frac{1}{2(1-\nu)} \sum_{k=1}^n \frac{\alpha_k}{\alpha_0} \left[1 + (1-2\nu) \frac{G_k}{G_0} \right] \right. \\ \left. \times \bar{\theta}_k(p) \right\} p^2 J_1(pr) dp, \end{aligned} \quad (21)$$

where \bar{w} is the Laplace transform of the axial displacement at the surface exposed to the power laser beam,

$$\bar{\theta}_0 = \int_{-\infty}^0 \bar{T}_0(z_0) \exp(pz_0) dz_0, \quad \bar{\theta}_k = \int_0^{\Delta_k} \bar{T}_k(z_0) dz_0. \quad (22)$$

Taking into account Eqs. 13, 14, and 22, we can rewrite Eq. 21 as follows:

$$\bar{\varepsilon}(r, s) = 4\alpha_0 (1 + \nu) \bar{f}(s) \int_0^\infty Q(p, s) p^2 J_1(pr) dp, \quad (23)$$

where

$$Q(p, s) = N_0 \left\{ \frac{1}{\gamma_0 + p} + \frac{1}{2(1 - \nu)} \sum_{k=1}^n \frac{\alpha_k}{\alpha_0} \left[1 + (1 - 2\nu) \frac{G_k}{G_0} \right] \frac{\Delta_k}{\mu_k} \right. \\ \left. \times [(1 - \exp(-\mu_k)) A_k + (\exp(\mu_k) - 1) B_k] \right\}. \tag{24}$$

In order to determine the inverse Laplace transform of Eq. 23, we use the decomposition theorem,

$$L^{-1} \left[\frac{\Phi(s)}{\Psi(s)} \right] = \sum_{s_m} \frac{\Phi(s_m)}{(\partial \Psi / \partial s)|_{s=s_m}} \exp(s_m t), \tag{25}$$

where s_m are the roots of the equation $\Psi(s_m) = 0$. The inverse Laplace transform of Eq. 23 contains the relaxation ε_{rel} and the “wave” ε_w components. The first component is determined by the branching points of the functions N_0 (see Eqs. 20 and 24) and does not depend on the frequency of modulation of the heating laser pulse. We are interested in the phase of the “wave” component ε_w (the principal measured parameter of the photothermal method) which is determined by simple poles s_m of the function $\bar{f}(s)$ (see Eqs. 10 and 23) which are located on the imaginary axis:

$$\Psi(s_m) = 1 - \exp[-s_m(\tau_0 + \tau)] = 0. \tag{26}$$

Solution of Eq. 26 reads

$$s_m = \pm im\omega, \quad m = 1, 2, 3 \dots n, \quad i = \sqrt{-1}, \tag{27}$$

except for the case when $\frac{2m\tau_0}{\tau_0 + \tau} = N$ is an integer, $\omega = 2\pi/(\tau_0 + \tau)$ is a cyclic frequency.

Let us determine the inverse Laplace transform of Eq. 23 using Eqs. 25 and 27. Substituting the roots s_m given by Eq. 27 into Eqs. 17–19, 23, and 25 yields

$$\varepsilon_w(r, t) = \frac{2\alpha_0(1 + \nu)}{\pi} \sum_{m=-\infty}^{\infty} \frac{[1 - \exp(-im\omega\tau_0)]}{m} \exp[i(m\omega t - \pi/2)] \int_0^{\infty} |Q(p, s_m)| \\ \times \exp(-i\delta_m) p^2 J_1(pr) dp. \tag{28}$$

Here

$$\varphi_k = \tan^{-1} \left(\frac{m\omega}{a_k p^2} \right), \quad \mu_k = \frac{p\Delta_k}{\sqrt{\cos \varphi_k}} [\cos(\varphi_k/2) + i \sin(\varphi_k/2)], \\ \delta_m = \tan^{-1} \left[\frac{\text{Im}(Q(p, s_m))}{\text{Re}(Q(p, s_m))} \right].$$

Taking into account that

$$\operatorname{Re} [Q (s_m)] = \operatorname{Re} [Q (-s_m)], \quad \operatorname{Im} [Q (s_m)] = -\operatorname{Im} [Q (-s_m)],$$

after some algebra, Eq. 28 can be rewritten as follows:

$$\begin{aligned} \varepsilon_w (r, t) = & \frac{8\alpha_0 (1 + \nu)}{\pi} \sum_{m=1}^{\infty} \frac{\sin (m\omega\tau_0/2)}{m} \int_0^{\infty} |Q (p, s_m)| \cos [m\omega (t - \tau_0/2) - \delta_m] \\ & \times p^2 J_1 (pr) dp. \end{aligned} \quad (29)$$

The “wave” component of the beam deflection angle ε_w given by Eq. 29 can be rewritten as

$$\varepsilon_w (r, t) = \sum_{m=1}^{\infty} E_m (r) \cos [m\omega (t - \tau_0/2) - \Delta\Phi_m], \quad (30)$$

where the expressions for the amplitude E_m and the phase shift $\Delta\Phi_m$ of the deflection angle ε_w are as follows:

$$E_m = \frac{8\alpha_0 (1 + \nu)}{\pi} \frac{\sin (m\omega\tau_0/2)}{m} \sqrt{I_c^2 + I_s^2}, \quad \Delta\Phi_m = \tan^{-1} \frac{I_s}{I_c}, \quad (31)$$

$$I_c = \int_0^{\infty} |Q (p, s_m)| \cos (\delta_m) p^2 J_1 (pr) dp, \quad (32)$$

$$I_s = \int_0^{\infty} |Q (p, s_m)| \sin (\delta_m) p^2 J_1 (pr) dp. \quad (33)$$

The amplitude E_m and the phase shift $\Delta\Phi_m$ in Eqs. 31–33 depend on the frequency ω and physical characteristics of a coating.

Let us determine the phase shift $\Delta\Phi_m$ in a particular case when a coating is removed ($\Delta = 0$). The temperature distribution in a substrate given by Eq. 14 reads

$$\bar{T}_0 = \frac{I_0 \sigma_0 r_0^2 \exp (-p^2 r_0^2 / 4) \exp (\gamma_0 z)}{2\lambda_0 [\gamma_0 + (\lambda_g / \lambda_0) \gamma_g]} \bar{f} (s). \quad (34)$$

Substituting Eq. 34 into Eq. 21 and, taking into account that $\lambda_g / \lambda_0 \ll 1$ (in the case of a metallic substrate), we arrive at the following expression for the beam deflection angle:

$$\begin{aligned} \varepsilon_w (r, t) = & \frac{4I_0 \sigma_0 r_0^2 \alpha_0 (1 + \nu)}{\pi \lambda_0} \sum_{m=1}^{\infty} \frac{\sin (m\omega\tau_0/2)}{m} \int_0^{\infty} R (p) \cos [m\omega (t - \tau_0/2) - \delta_m] \\ & \times J_1 (pr) dp, \end{aligned} \quad (35)$$

where

$$R(p) = \frac{\cos \varphi_0 \exp(-p^2 r_0^2/4)}{\sqrt{1 + 2\sqrt{\cos \varphi_0} \cos(\varphi_0/2) + \cos \varphi_0}}, \quad \varphi_0 = \tan^{-1} \left(\frac{m\omega}{a_0 p^2} \right), \quad (36)$$

$$\delta_m = \tan^{-1} \left(\frac{\sin \varphi_0 + \sqrt{\cos \varphi_0} \sin(\varphi_0/2)}{\cos \varphi_0 + \sqrt{\cos \varphi_0} \cos(\varphi_0/2)} \right), \quad I_c = \int_0^\infty R(p) \cos(\delta_m) J_1(pr) \, dp \quad (37)$$

$$I_s = \int_0^\infty R(p) \sin(\delta_m) J_1(pr) \, dp, \quad \Delta\Phi_m = \tan^{-1} \left(\frac{I_s}{I_c} \right). \quad (38)$$

In this case the phase shift $\Delta\Phi_m$ of the monitoring beam depends only on the thermal diffusivity a_0 . Equations 36–38 can be simplified for the high magnitude of the modulation frequency ω , i.e., for $\frac{a_0 p^2}{m\omega} \ll 1$:

$$\varphi_0 = \tan^{-1} \left(\frac{m\omega}{a_0 p^2} \right) \approx \frac{\pi}{2} - \frac{a_0 p^2}{m\omega}, \quad \Delta\Phi_m \approx \frac{\pi}{2} - \sqrt{\frac{2a_0}{m\omega}} \frac{I_3}{I_2}, \quad (39)$$

where

$$I_n = \int_0^\infty \exp(-p^2 r_0^2/4) (p)^n J_1(pr) \, dp.$$

Equation 39 implies that $\Delta\Phi_m \rightarrow \pi/2$ in the high modulation frequency range.

The measured photothermal signal by the position sensor expanded in harmonic series terms is determined by Eq. 30. The amplitude E_m and the phase shift $\Delta\Phi_m$ depend on the laser operating parameters (power I_0 , beam radius r_0), thickness of a coating and thermal characteristics of a coating and a substrate. Function $f(t)$ that describes the temporal dependence of the power $I(t)$ of a heating laser beam can be expanded in a Fourier series:

$$f(t) = L^{-1} [\bar{f}(s)] = \frac{\tau_0}{\tau_0 + \tau} + \frac{2}{\pi} \sum_{m=1}^\infty \frac{\sin(m\omega\tau_0/2)}{m} \cos[m\omega(t - \tau_0/2)]. \quad (40)$$

Equations 30 and 40 imply that the function $\Delta\Phi_m$ is the phase shift between beam power $I(t)$ and the monitoring beam deflection angle ε_w . Comparing the measured values of the amplitude E_m and the phase shift $\Delta\Phi_m$, corresponding to a frequency spectrum $m\omega (m = 1, \dots, n)$, with the theoretically predicted values from Eq. 30 it is possible to determine the physical characteristics of a coating. The amplitude E_m also depends on the laser beam parameters (power I_0 and beam radius r_0) and the surface reflectivity σ_0 which can be measured with the error depending on the experimental conditions. The latter decreases the accuracy of the photothermal method. The phase

$\Delta\Phi_m$ does not depend on I_0 and σ_0 . Besides, calculations show that the phase $\Delta\Phi_m$ is significantly more sensitive (in comparison with E_m) to variations of the physical characteristics and, therefore, is adopted as the principal measured parameter of the suggested method.

3 Results and Discussion

A typical photothermal displacement measuring device and the experimental configuration which employs the beam deflection scheme are described in [2]. The modulated pulse of a power laser is directed normally onto the specimen and causes the non-uniform heating and buckling of a coating–substrate assembly. The monitoring beam of a second laser is reflected from a coating at an angle ε that depends on the temperature and strain fields and, consequently, upon the physical properties of a specimen. The periodic change of the temperature and displacement of a coating cause a periodic change of the deflection angle ε that is registered by a sensitive position sensor. Usually, the photothermal displacement is a small perturbation of the irradiated surface. When the temperature rise $T_1(r = 0, z = \Delta)$ is of the order of 10 K, the maximum value of the deflection angle is of the order of 10^{-6} rad which can be registered by a standard device (Olmstead et al. [2] measured a slope of 10^{-8} rad). The monitoring laser beam is divided into two parallel beams: the first beam strikes the specimen at $r = 0$ (axis of a power laser beam) while the second beam strikes at a distance r from the axis. If the optical system is positioned precisely, the deflection angle of the first (reference) beam does not change during the stage of heating of the specimen, and the second beam is reflected at a different angle measured by the position sensor. The beam deflection angle ε which is a principal measured parameter of the photothermal method, is determined by the following relation:

$$\varepsilon = \frac{d - d_0}{L}, \quad (41)$$

where d_0 and d are the distances measured by the position sensor between the two monitoring beams before and during the stage of heating, respectively, and L is the distance from the specimen to the sensor. This scheme which employs the reference monitoring beam increases the accuracy of measurements.

The signal registered by the position sensor is stored in a computer for further Fourier analysis based on the known modulation frequency ω . As a result of the analysis, the beam deflection angle is obtained in the following form:

$$\varepsilon_w = \sum_{m=1}^{\infty} E'_m \cos [m\omega (t - \tau_0/2) - \Delta\Phi'_m]. \quad (42)$$

Here E'_m and $\Delta\Phi'_m$ are the amplitude and phase shift of the beam deflection angle obtained by Fourier analysis of experimental data. The theoretical values of the phase shift $\Delta\Phi_m$ are determined in Eq. 30. The physical characteristics of a coating can be determined by fitting the experimental and theoretical values of $\Delta\Phi_m$. Equation 30

includes several parameters, e.g., thermal diffusivity, thermal conductivity, linear thermal expansion coefficient, coating thickness, etc., which are not known with high precision. These parameters are determined by fitting the experimental data to the calculated values using an algorithm described in [11].

The suggested procedure for determining the physical characteristics of a coating comprises the following stages:

- (a) Measuring the phase shift $\Delta\Phi_m$ for a substrate (without a coating) by a photo-thermal method and determining the thermal diffusivity a_0 using Eqs. 35–38. The calculated value of thermal diffusivity a_0 is compared with the results obtained previously by traditional experimental methods. This allows determining the accuracy of the photothermal method and checking positioning of the power and monitoring laser beams.
- (b) Determining physical characteristics (a_k, λ_k, α_k) after deposition of every individual layer of a coating beginning with a first layer deposited on a substrate and ending with the external layer. Since physical characteristics vary from layer to layer, the surface displacement w_n , the monitoring beam deflection angle ε_w and, consequently, the phase shift $\Delta\Phi_m$ change with increasing number of layers in a coating. Therefore, by measuring the phase shift before and after deposition of a layer k and, comparing the results of measurements with theoretical predictions, allows determining physical properties of this layer.

Assume that the parameters of a repetitive laser beam are as follows: the normalized pulse duration $\tau_0/(\tau_0 + \tau) = 1/3$, $r_0 = 1$ mm, the rest of the parameters do not influence $\Delta\Phi_m$. In this study we considered the following assemblies:

- Assembly #1 - Three-layer coating deposited on a Ni substrate. The coating is composed of the compound ZrO₂ (20 vol%) + Ni (80 vol%), ZrO₂ (40 vol%) + Ni (60 vol%) and ZrO₂ (80 vol%) + Ni (20 vol%) for the internal ($k = 1$), intermediate ($k = 2$), and external layers ($k = 3$), respectively. This assembly is characterized by a low thermal conductivity of a coating and a high thermal conductivity of a substrate.
- Assembly #2 - Three-layer coating deposited on a high-speed (HS) steel substrate. The coating is composed of the compounds WC (20 vol%) + steel (80 vol%), WC (40 vol%) + steel (60 vol%), and WC (80 vol%) + steel (20 vol%) for the internal, intermediate, and external layers, respectively. The thermal characteristics of a coating and a substrate are of the same order (see Table 1). The values of the properties of metals in the substrates which are used in computations are given in [14]. Physical properties of the composite materials constituting the coatings are calculated as the volume averaged values [15].

Consider the results obtained for these assemblies. For the purpose of illustration of the results we use the difference $\Phi_m = (\pi/2 - \Delta\Phi_m)$ instead of $\Delta\Phi_m$. Numerical results are obtained for the distance between the power laser beam and the monitoring beam axes $r = 1$ mm and 2 mm for assemblies #1 and #2, respectively. Figures 2 and 3 show the dependencies of the phase shift Φ_m ($m = 1, 2$) versus the thickness Δ_k ($k = 1, 2, 3$) for assemblies #1 and #2, respectively. Curves

Table 1 Thermophysical and mechanical properties of materials

Material	λ ($\text{W} \cdot \text{m}^{-1} \cdot \text{K}^{-1}$)	a ($10^{-6} \text{m}^2 \cdot \text{s}^{-1}$)	α (10^{-6}K^{-1})	G (GPa)
Ni	69	15.0	15.5	78
ZrO ₂ (20 vol%)/Ni	9.0	1.92	14.4	77
ZrO ₂ (40 vol%)/Ni	4.8	1.0	13.3	76
ZrO ₂ (80 vol%)/Ni	2.48	0.5	10.8	75
HS steel	31	4.8	13	77
WC(20 vol%)/steel	32.5	5.5	8.6	120
WC(40 vol%)/steel	34.1	6.3	6.6	162
WC(80 vol%)/steel	37.8	8.8	5.3	218

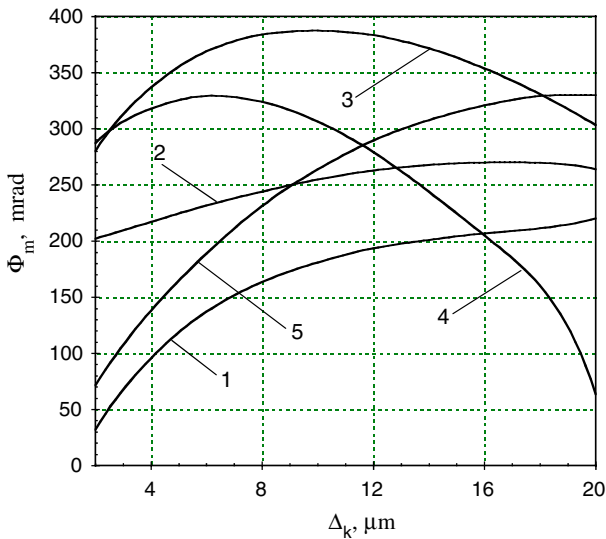


Fig. 2 Dependence of the phase shift Φ_m versus thickness Δ_k of ZrO₂/Ni coating for two modulation frequencies, 5 kHz (curves 1–4) and 2 kHz (curve 5). Curve 1—one-layer coating, $m = 1$; Curve 2—two-layer coating, $\Delta_1 = 10 \mu\text{m}$, $m = 1$; Curves 3, 5—three-layer coating, $\Delta_1 = \Delta_2 = 10 \mu\text{m}$, $m = 1$; and Curve 4—three-layer coating, $m = 2$

1 and 2 are obtained for a one-layer coating ($k = 1$), curves 3, 4—for a two-layer coating ($\Delta_1 = 10 \mu\text{m}$, $k = 2$), curves 5, 6—for a three-layer coating ($\Delta_1 = \Delta_2 = 10 \mu\text{m}$, $k = 3$). Calculations showed that the phase shift changes significantly with increasing number of layers m deposited at a substrate (especially, for assembly #1). For example, after deposition of the external layer with the thickness $\Delta_3 = 4 \mu\text{m}$, the phase shift increases from 255 mrad to 338 mrad (see Fig. 2, curves 2 and 3). Therefore, the proposed photothermal method can be used for measuring properties of thin layers. Calculations performed for assembly #1 showed that the phase shift is a non-monotonic function of the thickness Δ_k . The phase shift increases for small values of Δ_k and decreases with increase in the thickness (curves 1 and 2 attain the

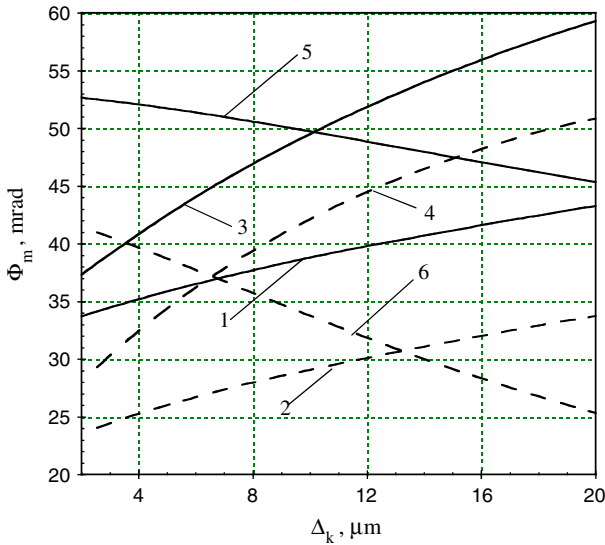


Fig. 3 Dependence of the phase shift Φ_1 (solid lines) and Φ_2 (dashed lines) versus thickness Δ_k of WC/steel coating for $\omega = 5$ kHz. Curves 1, 2—one-layer coating, Curves 3, 4—two-layer coating, and Curves 5, 6—three-layer coating

maximum values for $\Delta_1, \Delta_2 \approx 25 \mu\text{m}$). The obtained values of the phase shift are sufficiently large and can be registered by commercially available devices. In order to obtain higher magnitudes of the phase shift in the case of a thickness $\Delta_k > 30 \mu\text{m}$, it is necessary to decrease the modulation frequency ω (see curve 2, Fig. 2) of a heating laser beam. In the case of assembly #2, the dependence $\Phi_m(\Delta_k)$ is more involved. The phase shift Φ_m is significantly lower for assembly #2 in comparison with assembly #1 because the thermophysical characteristics of a coating and a substrate for assembly #2 are close, and deposition of the additional layer only weakly affects the temperature distribution in the assembly. The maximum magnitude of Φ_m strongly depends on the modulation frequency ω . In the case of assembly #2, the phase shift Φ_m is an increasing function of Δ_k for one- and two-layer coatings (see curves 1–4, Fig. 3) and is a decreasing function for a three-layer coating (see curves 5 and 6, Fig. 3). Therefore, it is desirable to decrease the modulation frequency as the number of the deposited layers in a coating increases. We investigated the dependence of the phase shift on the modulation frequency ω (curves 1–4 and 5 in Fig. 3 are obtained for three- and two-layer coatings, respectively). It was found that the function Φ_m decreases with increase of the modulation frequency ω (see Fig. 4), and an especially sharp decrease occurs in the frequency range $\omega > 20$ kHz in the case of a three-layer coating (see curves 1–4 in Fig. 4). In a high frequency range $\omega > 100$ kHz, the phase shift Φ_m tends to zero (similarly to a case without a coating) regardless of the thermal characteristics of a coating, and the sensitivity of the phase measurement sharply decreases. Therefore, it is desirable to perform the photothermal experiment in the range of moderate modulation frequencies, $\omega < 20$ kHz.

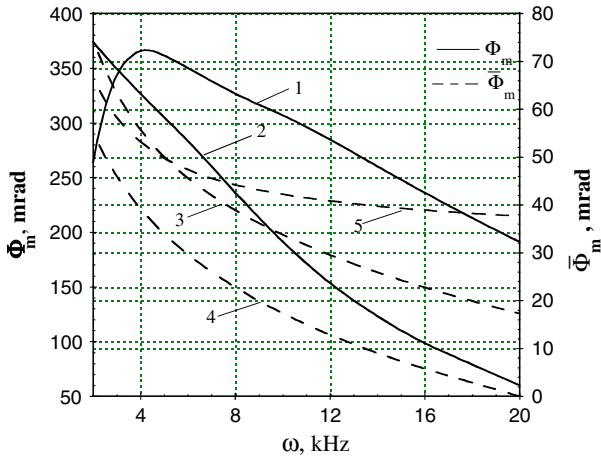


Fig. 4 Dependence of phase shift Φ_m and $\bar{\Phi}_m$ versus modulation frequency ω for ZrO₂/Ni (curves 1, 2) and WC/steel (curves 3–5) coatings, respectively. Curves 1, 3, 5— $m = 1$, Curves 2, 4— $m = 2$

We studied also the sensitivity of the phase measurements to variations of thermal diffusivity a/a_3 , thermal conductivity λ/λ_3 , and the coefficient of linear thermal expansion α/α_3 of the external ($k = 3$) layer of a coating (a , λ , α are varied values of thermal diffusivity, thermal conductivity, and coefficient of linear thermal expansion, respectively). Thermal characteristics a_3 , λ_3 , α_3 are reported in Table 1, the remaining parameters are as follows: the frequency $\omega = 10$ kHz, the thickness of the layers $\Delta_1 = \Delta_2 = \Delta_3 = 10 \mu\text{m}$, and the normalized pulse duration $\tau_0/(\tau_0 + \tau) = 1/3$. One of the characteristics is varied in the range $0.5 < a/a_3, \lambda/\lambda_3, \alpha/\alpha_3 < 1.5$, while the remaining two characteristics remains unchanged. Calculations showed that the phase shift Φ_m is very sensitive to variations of the physical characteristics, especially, variations of a/a_3 and α/α_3 (see Figs. 5, 6). It has been found that a maximum of sensitivity of the phase shift Φ_m to variations of the physical characteristics is achieved in the frequency range $5 \text{ kHz} < \omega < 20 \text{ kHz}$ and $1 \text{ kHz} < \omega < 20 \text{ kHz}$ for assemblies #1 and #2, respectively. In the low frequency range $\omega < 1 \text{ kHz}$, the values of the phase shift Φ_m are larger than in a range $1 \text{ kHz} < \omega < 20 \text{ kHz}$, but the sensitivity of Φ_m to variations of the thermophysical properties in a low frequency range sharply decreases. For example, the values of the phase shift for assembly #2 are $\Phi_m = (140.2, 100.7, \text{ and } 100.4) \text{ mrad}$ for $\omega = 1 \text{ kHz}$ and $\Phi_m = (172, 33.7, \text{ and } -1) \text{ mrad}$ for $\omega = 10 \text{ kHz}$ for three different values of the thermal diffusivity, $a/a_3 = 0.5, 1, \text{ and } 1.5$, respectively (see Fig. 6). Clearly the frequency $\omega = 10 \text{ kHz}$ is preferable to the frequency 1 kHz . In spite of the relatively large values of the phase shift Φ_m in a frequency range $\omega < 1 \text{ kHz}$, the sensitivity of the method in this frequency range is low. On the other hand, we found that the sensitivity significantly decreases for $\omega > 20 \text{ kHz}$. For example, the phase shift Φ_1 varies (due to variation of the thermal diffusivity a/a_3 , see Fig. 5) from 500 mrad to 217 mrad at $\omega = 10 \text{ kHz}$ and from 230 mrad to 133 mrad at $\omega = 20 \text{ kHz}$. Consequently, the photothermal experiment should be performed in a range of moderate modulation frequencies $1 \text{ kHz} < \omega < 20 \text{ kHz}$. In the high frequency range

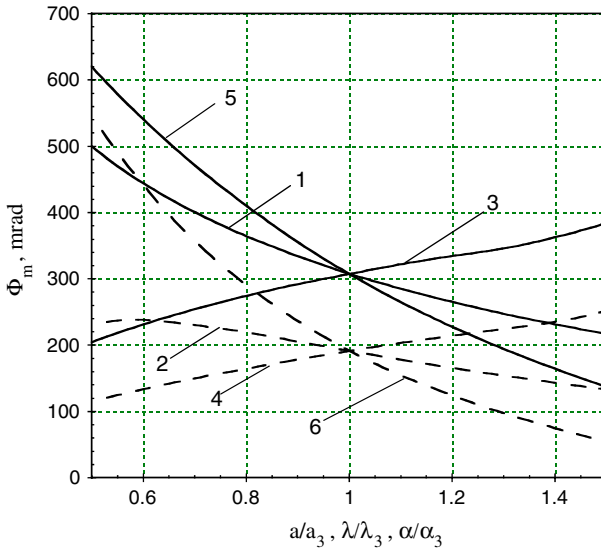


Fig. 5 Phase shift Φ_1 (curves 1, 3, 5) and Φ_2 (curves 2, 4, 6) as functions of normalized thermal characteristics a/a_3 (curves 1, 2), λ/λ_3 (curves 3, 4), and α/α_3 (curves 5, 6) for a three-layer ZrO_2/Ni coating

$\omega > 100 \text{ kHz}$ the phase shift Φ_m tends to zero (similarly to a case without a coating) independent of the magnitudes of the thermal characteristics of a coating, and the sensitivity of the phase measurement sharply decreases. Calculations conducted for one-, two-, and three-layer coatings showed that the sensitivity of the phase measurements to variations of physical properties decreases as the number of layers in a coating increases. In order to overcome this tendency, it is desirable to reduce the modulation frequency ω of the heating laser beam as the number of layers increases.

We compared the computed phase shift Φ_m of the deflection angle ε with the experimental values of the phase of the surface temperature obtained for a two-layer coating (Ni/SiO_2)-substrate (Si) assembly in a range of modulation frequency $2 \text{ kHz} < \omega < 20 \text{ kHz}$ [16]. These experimental results are obtained using the method of photoacoustic spectroscopy that is based on the modulated heating of the sample surface. As a result, the acoustic waves propagate in the gas cell. Measurements of the pressure of the acoustic waves allow determination of the phase data of the modulated *one-dimensional* temperature rise of the sample surface. In the present study we obtained the phase shift in a case of the *two-dimensional* temperature rise. It must be emphasized that in this case application of the photoacoustic spectroscopy method is much more involved because of the convective flow of gas along the sample surface caused by a non-uniform temperature distribution. Consequently, the comparison between the theoretical values of the phase shift $\Delta\Phi_m$ (see Eq. 31) and the experimental results is indirect and only qualitative. Nevertheless, experimental data show that the phase shift changes from -520 mrad to -310 mrad when the frequency is increased from 2 kHz to 20 kHz [16], while the calculated values of the phase shift change from -205 mrad to 31 mrad . In both cases the phase shift is an increasing function of frequency.

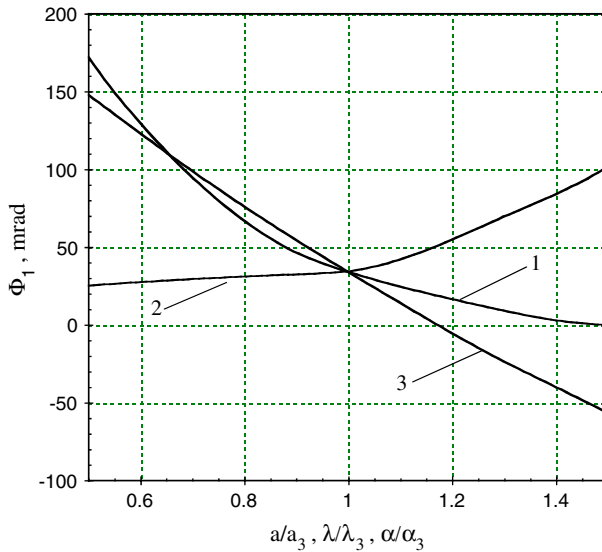


Fig. 6 Phase shift Φ_1 as function of normalized thermal characteristics a/a_3 (curve 1), λ/λ_3 (curve 2), and α/α_3 (curves 3) for a three-layer WC/steel coating

Hence, the obtained theoretical results are in qualitative agreement with experimental results.

4 Conclusions

We described a methodology and theory of the photothermal displacement method for measuring thermal characteristics of multilayer and FGM coatings. To this end, a coating is irradiated by repetitive pulses of a pump laser resulting in buckling of an illuminated surface due to non-uniform thermal expansion of a coating–substrate assembly. The monitoring beam of another laser is directed onto the heated surface and reflected from it at a different angle ε (the principal measured parameter of the method) depending on time and physical properties of a coating and a substrate. The beam deflection angle is registered by a sensitive detector, and the obtained signal is expanded in a Fourier series in order to determine the phase shift Φ_m (m is an ordinal number of harmonics) between the power of a heating laser beam and the monitoring beam deflection angle. We solved equations of thermal elasticity for a multilayer coating–substrate assembly heated by repetitive pulses of a pump laser using the Laplace–Hankel transform and developed the recursion procedure for determining the temperature field in the assembly, the displacement of the irradiated surface of a coating and the phase shift Φ_m . Thermal properties of the coating can be determined by comparing the experimentally measured values of the phase shift with the predicted theoretical values Φ_m . It was shown that the phase shift Φ_m is very sensitive to variations of thermal characteristics, especially the thermal diffusivity and thermal expansion coefficient. We determined the range of modulation frequencies (1 kHz to

20kHz) of the repetitive laser pulses whereby the sensitivity of the suggested method for measuring thermal properties is maximum.

References

1. D.P. Almond, P.M. Patel, *Photothermal Science and Techniques* (Chapman and Hall, London, 1996), pp. 63–98
2. M.A. Olmstead, N.M. Amer, S. Kohn, D. Fournier, A.C. Boccara, *Appl. Phys. A: Mater. Sci. Process.* **32**, 141 (1983)
3. P. Zimmermann, D. Ristau, E. Welsch, *Appl. Phys. A: Mater. Sci. Process.* **58**, 377 (1994)
4. G.L. Bennis, R. Vyas, R. Gupta, S. Ang, W.D. Brown, *J. Appl. Phys.* **84**, 3602 (1998)
5. A. Neubrand, H. Becker, T. Tschudi, *J. Mater. Sci.* **38**, 4193 (2003)
6. J. Opsal, A. Rosencwaig, *J. Appl. Phys.* **53**, 4240 (1982)
7. A. Rosencwaig, *J. Appl. Phys.* **49**, 2905 (1978)
8. J. Balderas-Lopez, A. Mandelis, *Rev. Sci. Instrum.* **74**, 5219 (2003)
9. Y. Nagasaka, T. Sato, T. Ushiku, *Meas. Sci. Technol.* **12**, 2081 (2001)
10. C.D. Martinsons, A.P. Levick, G.J. Edwards, *Int. J. Thermophys.* **24**, 1171 (2003)
11. H. Machlab, W.A. McGahan, J.A. Woollam, K. Cole, *Thin Solid Films* **224**, 22 (1993)
12. A.C. Boccara, D. Fournier, J. Badoz, *Appl. Phys. Lett.* **36**, 130 (1980)
13. T. Elperin, G. Rudin, *Int. J. Thermophys.* **28**, 60 (2007)
14. Y.S. Touloukian, R.K. Kirby, R.E. Taylor, T.Y. Lee (eds.), *Thermophysical Properties of Matter* (IFI/Plenum, New York, 1972)
15. T. Elperin, G. Rudin, *Heat Mass Transf.* **38**, 625 (2002)
16. H. Hu, X. Wang, X. Hu, *J. Appl. Phys.* **86**, 3953 (1999)